Classification: BIOLOGICAL SCIENCES: Microbiology

Title: Synergistic malaria vaccine combinations identified by systematic antigen screening

Short title: Blood-stage malaria vaccine combinations

Authors:

Leyla Y. Bustamante[a]†‡, Gareth T. Powell[b]†‡, Yen-Chun Lin[c], Michael D. Macklin[d], Nadia Cross[a], Alison Kemp[a], Paula Cawkill[a], Theo Sanderson[a], Cecile Crosnier[b], Nicole Muller-Sienerth[c], Ogobara K. Doumbo[e], Boubacar Traore[e], Peter D. Crompton[f], Pietro Cicuta[c], Tuan M. Tran[d], Gavin J. Wright[c], Julian C. Rayner[a*]

Affiliations:

[a]Malaria Programme, Wellcome Trust Sanger Institute, Wellcome Genome Campus, Cambridge CB10 1SA, United Kingdom.

[b]Cell Surface Signalling Laboratory, Wellcome Trust Sanger Institute, Wellcome Genome Campus CB10 1SA, Cambridge, United Kingdom.

[c]Cavendish Laboratory, University of Cambridge, Cambridge CB3 0RS, United Kingdom

[d]Division of Infectious Diseases, Department of Medicine, Indiana University School of Medicine, Indianapolis, IN 46202, United States

[e]Mali International Center of Excellence in Research, University of Sciences, Techniques and Technologies of Bamako, 1805 Bamako, Mali

[f]Laboratory of Immunogenetics, National Institute of Allergy and Infectious Diseases, National Institutes of Health, Rockville, MD 20892, United States

*To whom correspondence should be addressed: Julian Rayner, Malaria Programme, Wellcome Trust Sanger Institute, Wellcome Genome Campus, Cambridge CB10 1SA, United Kingdom. Phone: +44 1223 492327. e-mail: julian.rayner@sanger.ac.uk.

†Contributed equally to this work

‡Current addresses:

L. Y. B: : Ferrier Research Institute, Chemical Biology Laboratory, Kelburn Parade, Victoria University of Wellington, PO Box 600, Wellington 6140, New Zealand.

G. T. P.: Department of Cell and Developmental Biology, University College London, Gower St., London, WC1E 6BT, United Kingdom.

Keywords: Malaria, vaccine, *Plasmodium falciparum*, antigen combinations, erythrocyte invasion

Abstract

A highly effective vaccine would be a valuable weapon in the drive towards malaria elimination. No such vaccine currently exists, and only a handful of the hundreds of potential candidates in the parasite genome have been evaluated. In this study we systematically evaluated twenty-nine antigens likely to be involved in erythrocyte invasion, an essential developmental stage during which the malaria parasite is vulnerable to antibody-mediated inhibition. Testing antigens alone and in combination identified several strain-transcending targets that had synergistic combinatorial effects *in vitro*, while studies in an endemic population revealed that combinations of the same antigens were associated with protection from febrile malaria. Video microscopy established that the most effective combinations targeted multiple discrete stages of invasion, suggesting a mechanistic explanation for synergy. Overall, this study both identifies specific antigen combinations for high priority clinical testing, and establishes a generalizable approach that is more likely to produce effective vaccines.

Significance Statement

Malaria still kills hundreds of thousands of children each year. Malaria vaccine development is complicated by high levels of parasite genetic diversity, which makes single target vaccines vulnerable to the development of variant-specific immunity. To overcome this hurdle, we systematically screened a panel of twenty-nine blood stage antigens from the most deadly human malaria parasite, *Plasmodium falciparum.* We identified several new targets that were able to inhibit erythrocyte invasion in two genetically diverse strains. Testing these targets in combination identified several pairs that blocked invasion more effectively in combination than in isolation. Video microscopy and studies of natural immune responses to malaria in patients suggests that targeting multiple steps in invasion is more likely to produce a synergistic vaccine response.

\body

Introduction

Plasmodium falciparum malaria remains one of the most significant global public health challenges, with more than 200 million cases and 438,000 deaths in 2015 (1). There has recently been significant process in reducing malaria mortality (2), but the emergence and spread of parasites resistant to current frontline antimalarial artemisinin (3) threaten current control methods and emphasize the need for novel control and intervention tools, such as an effective vaccine. Malaria vaccine development has been challenging, with only one vaccine, RTS,S (Mosquirix), reaching Phase III trials where it had limited, albeit consistent, efficacy (4). While the WHO has recommended that RTS,S be advanced to large-scale pilots in Africa, the well-established partial efficacy coupled with concerns about strain-specific responses (5) makes identifying additional components to include in a second-generation *P. falciparum* vaccine an urgent priority.

Two significant challenges confront *P. falciparum* antigen identification - the complexity of the parasite life cycle which presents a large number of potential targets, and the depth of genomic diversity across global parasite populations (6) which makes the development of strain-transcending protection difficult. Given these twin challenges, an effective second-generation vaccine will almost certainly need to target multiple components simultaneously (7). Despite this fact, malaria vaccine development has so far primarily focused on a very limited number of targets, leaving the vast majority of potential candidates encoded by the >5,000 gene *P. falciparum* genome unexplored (8). The search for vaccines targeting erythrocyte invasion is a microcosm of this broader challenge. Erythrocyte invasion, the process by which *P. falciparum* merozoites recognise, form protein-protein interactions with, and then actively invade human erythrocytes, is essential for parasite survival and is the only window during blood stage

development when the parasite is extracellular and therefore exposed to antibody-mediated inhibition. It is also a very complex process, potentially involving more than 400 genes, including more than 100 that may encode for surface exposed proteins (9). Until now however, invasion blocking vaccines have focused on only a handful of targets, which not coincidentally were also among the first *P. falciparum* genes ever sequenced (8).

A reverse vaccinology approach will be needed to identify new targets from this long candidate list, incorporating systematic screens of larger number of antigens and using data from multiple sources to identify potentially synergistic combinations. We have previously used a mammalian expression system to express a library of entire ectodomains, up to 200kDa in length, from merozoite expressed *Plasmodium* proteins that are thought to be involved in erythrocyte recognition and entry (10). Expressing full-length protein ectodomains in the context of a eukaryotic secretory pathway allows disulphide bonds to form and maximizes the chance that the recombinant antigens will fold correctly to mimic the function and antigenicity of native *P. falciparum* proteins, all of which pass through the *P. falciparum* secretory pathway. This library has been used to identify new protein-protein interactions (11), perform detailed biochemical analysis of known interactions (12), and underpin large-scale immuno-epidemiological studies to identify targets of protective immunity (13). In this study we tested whether this ectodomain library could be used to identify new erythrocyte invasion-blocking vaccine combinations by raising antibodies against multiple *P. falciparum* proteins, systematically testing their ability to inhibit invasion, and incorporating immunoepidemiological and mechanistic data to identify synergistic combinations.

Results

Systematic screening identifies novel strain-transcendent vaccine candidates

The extracellular domain of each target protein, based on sequence from the reference 3D7 *P. falciparum* genome, was produced in a soluble recombinant form by transient transfection of HEK239E cells (14). We down-selected 29 targets for further investigation, based both on the diversity of their known or inferred sub-cellular location, and on pragmatic considerations such as protein expression level (Table S1, Fig S1). 0.4-1.0 mg of each protein was purified using nickel affinity chromatography, and used to raise polyclonal rabbit antibodies. Total IgG antibodies were purified using Protein G columns and tested by ELISA to confirm binding activity against the immunizing antigens (Fig S2) before being used in growth inhibition activity (GIA) assays.

To establish whether each antibody alone could inhibit parasite growth, late trophozoite stage *P. falciparum* parasites were cultured in the presence of IgG at the maximum concentration that could be purified from the polyclonal antisera. Parasites were incubated with each IgG for 24 hours to allow sufficient time for erythrocyte invasion to occur, before parasitemia was measured using flow cytometry (15). Antigen polymorphism has been a major cause of failure for previous *P. falciparum* candidate antigens. In order to incorporate testing for strain-transcending inhibition at the earliest stage of candidate down-selection, antibodies against all 29 targets were tested against both 3D7 and Dd2 parasites, which have genome sequences broadly representative of West African and Asian *P. falciparum* parasites respectively, and differ at >15,000 nucleotide positions across the 23Mb genome (16). IgG purified from polyclonal antibodies raised against PfRh5, a leading strain-transcending blood-stage vaccine candidate (17, 18), was used as a comparator in this and subsequent experiments. Antibodies raised against the 3D7 variants of PfMSP1, PfSERA9, PfMSRP5, PfEBA181, PfCyRPA and PfRAMA

all had a strong inhibitory effect on the growth of both 3D7 and Dd2 parasites, inhibiting 3D7 growth to a similar extent as anti-PfRh5 antibodies (Fig 1). PfEBA181, PfMSRP5 and PfSERA9 are members of gene families in which at least one other gene is known or suspected to play a role in erythrocyte invasion (PfMSP7-like (19), EBL (20), PfSERA (21)), so the inhibitory effects of each of these antibodies could in part be explained by cross-reactivity against multiple members of each protein family. We therefore tested the ability of the purified IgG for each of these proteins to recognise other members of each family, but only in the case of PfMSRP5-specific IgG was there any evidence for cross-reactivity (Fig S3), suggesting the IgG responses are largely target-specific. PfCyRPA is a member of a protein complex that includes PfRh5 (22, 23), while little is known about the function of PfRAMA, although antibodies against it have previously been associated with protection against malaria (24). PfMSP1 is an extensively studied vaccine target with known allele-specific effects (25), so was excluded from further study.

In order to quantitatively compare the inhibitory potential of IgG specific for the remaining five targets, GIA assays were performed using increasing concentrations of purified IgG to generate IC_{50} values. All exhibited a clear dose-dependent inhibitory effect on the growth of both 3D7 and Dd2 parasites (Fig S4); with IC_{50} values ranging from 0.25 mg/mL to 1.5 mg/mL total IgG (Table S2). Antibodies raised against PfSERA9, PfMSRP5 and PfRh5 did not show any evidence of strain specificity, with almost no difference in IC_{50} values between the two strains. Antibodies against PfEBA181, PfCyRPA and PfRAMA all showed some reduction in efficacy against Dd2 relative to 3D7 parasites, with an accompanying 1.7-fold (PfCyRPA and PfRAMA) and 2.7 fold (PfEBA181) increase in IC_{50} values. However, the difference in IC_{50} values for PfCyRPA and PfRAMA against 3D7 and Dd2 parasites was relatively minor and of a similar magnitude to shifts in IC_{50} values between different strains for anti-PfRh5 antibodies (18); and moreover,

PfCyRPA has previously been reported to have broadly strain-transcendent effects (22, 26). Strain-specificity is therefore only an immediate concern in the case of PfEBA181.

Candidates identified in vitro *are associated with protection from clinical malaria* in vivo

Repeated exposure to *P. falciparum* malaria generates immune responses to a large number of antigens (13, 27), which can result in clinical immunity. To investigate whether antibodies to these new vaccine targets contribute to clinical immunity we tested for the presence of naturally acquired IgG in uninfected Malian individuals enrolled in a prospective cohort study in which we previously described an association between PfRh5-specific IgG and protection from febrile malaria (28). At the uninfected baseline before the 6-month malaria season antigen-specific IgG levels and seroprevalence increased with age for all antigens except for PfCyRPA, which demonstrated poor natural immunogenicity, similar to its binding partner PfRh5 (Fig 2A, B). We next evaluated whether these baseline IgG levels predicted protection from febrile malaria during the ensuing malaria season. Associations between risk of febrile malaria, as measured by time-to-first febrile malaria episode after incident blood-stage infection, and IgG levels for each antigen, alone and in combination, were examined using a Cox regression model that included age, sickle cell trait, gender, and anemia as covariates. Although IgG specific for PfCyRPA, PfEBA181, PfMSRP5, PfRAMA or PfSERA9 did not predict protection individually, the combined presence of IgG specific for PfEBA181, PfMSRP5, or PfRAMA with PfRh5-specific IgG was associated with reduced malaria risk relative to PfRh5-specific IgG alone, albeit with overlapping confidence intervals (Table S3). A significantly reduced hazard ratio for the anti-PfEBA181 IgG + anti-PfRH5 IgG combination relative to anti-PfEBA181 IgG alone suggests that antibodies generated against these two antigens may provide malaria-protective synergy (Table S3). Notably, two combinations that did not contain anti-PfRh5 IgG (anti-PfEBA181 IgG + anti-PfMSRP5 IgG + anti-PfRAMA IgG and anti-PfMSRP5 IgG + anti-PfRAMA IgG) also predicted protection from malaria (Table S3). The protective effect of anti-PfEBA181

IgG + anti-PfMSRP5 IgG + anti-PfRAMA IgG, but not PfMSRP5 IgG + anti-PfRAMA IgG, remained significant even after controlling for reactivity against other *P. falciparum* antigens, including PfRh5 (Fig 2C). To determine whether positive IgG responses affected parasite growth, we compared *in vivo* parasite multiplication rates between negative and positive responders for each antigen combination among individuals for whom parasite density data was available. Although IgG responses to PfMSRP5 + PfRh5 and PfRAMA associated with lower parasite multiplication rates in univariate analyses, these associations were not significant after adjusting for multiple testing or in logistic regression models that included age, sickle cell trait, anemia and gender as covariates (Table S4).

Combining targets at multiple steps of invasion can increase synergy

These data suggest that IgG responses to these antigens contribute to naturally acquired immunity to malaria, and also suggest that combining these antigens in a vaccine could improve protective efficacy. We therefore assessed whether combining purified total IgG from different targets could act synergistically to inhibit parasite growth *in vitro.* The amount of anti-PfRAMA IgG was limiting, so we were only able to test this antibody in combination with anti-PfRh5 and anti-PfCyRPA IgG. Antibody interactions were evaluated over a range of concentrations by a fixed-ratio method (29) and IC_{50} values were used to calculate the 50% fractional inhibitory concentration (FIC_{50}). FIC_{50} values at different concentration ratios were used to construct isobolograms for each antibody combination (Fig 3). Several combinations of antibodies showed deviations from the diagonal line that would indicate purely additive interaction under Loewe additivity. Combinations of anti-PfCyRPA/PfSERA9, anti-PfCyRPA/PfRAMA, anti-PfRh5/PfRAMA and anti PfRh5/PfMSRP5 all showed deviations below the diagonal, indicating a trend towards synergy (Fig 3C, F, G, H), whereas the combinations of anti-PfEBA181/PfCyRPA and anti-PfEBA181/PfSERA9 showed curves above the diagonal, indicating a trend towards antagonism (Fig 3A, E). Several combinations of antibodies with anti-PfRh5 had different effects

at high and low concentrations of anti-PfRh5 (FIC_{50}>1) (Fig 3 D, I, J), emphasizing that the ratio in which two antibodies are combined can determine whether a given combination has a greater effect than that achieved by each antibody alone. To test the statistical significance of these interactions, we calculated an interaction index for each combination and modelled its associated 95% confidence interval (CI) using Monte Carlo simulation of the measurement errors in the IC_{50} values (Figure S5). This analysis showed no combination had CIs that did not include 1 at all concentrations tested, meaning that none were unfailingly either synergistic or antagonistic. However, the combinations of anti-PfRh5/PfRAMA and anti-PfCyRPA/PfRAMA were those with the most consistently synergistic interactions, while as noted above, several combinations including anti-PfRh5 combinations were significantly synergistic at low concentrations of anti-PfRh5, but not high concentrations (Figure S5). Combinations that included PfMSRP5 had particularly wide confidence intervals, decreasing the statistical weight that can be put to them.

One potential explanation for the combinatorial effects observed is that simultaneously blocking targets that act at different steps during invasion may not have the same effect as blocking targets that act at the same step of invasion. While the specific function of PfRh5 during invasion has been studied in detail (30), the role of the other antigens is much less well-defined. We therefore carried out video microscopy studies, incubating purified late schizonts from the 3D7 *P. falciparum* strain with purified IgG at the maximal concentration for each target. Schizont egress and subsequent merozoite-erythrocyte interactions were recorded using a recently described imaging platform (31), and multiple invasion associated parameters were quantified from these videos. All antibodies decreased the number of merozoite-erythrocyte contacts made after each egress, but anti-PfMSRP5 had the most significant effect at this very early stage of invasion (Fig 4A, Movies S1, S2), consistent with its presence on the merozoite surface. Anti-PfEBA181 was the only IgG that had a marked effect on prolonging the duration of merozoite-

erythrocyte interactions (Fig 4B, Movie S3), suggesting that it acts after the initial contact has occurred but before active invasion has begun, as has been suggested for other members of the same family of invasion ligands (30). By contrast, anti-PfRh5, PfCyRPA and PfSERA9 had no effect on the duration of contacts, but did have a significant effect on the severity of erythrocyte deformations (Fig 4C, Movies S4-6), with the majority of merozoites inducing little to no deformation (Fig 4D). Action at this late stage of invasion, interpreted as representing tight junction formation, has been previously reported for PfRh5 (30). Finally, anti-PfRAMA IgG had no effect on the number or severity of deformation events, (Fig 4D, E; Movie S7), indicating that it inhibits invasion much later in the process after the tight junction has been established. Taking the data together, these targets seem to function at discrete temporal steps during invasion, as summarized in Figure 4: 1) PfMSRP5, 2) PfEBA181, 3) PfRh5/PfCyRPA/PfSERA9, 4) PfRAMA. It is notable that combinations of antibodies that target both steps 3 and 4 (PfRh5/PfRAMA and PfCyRPA/PfRAMA) were the most consistently synergistic in GIA assays. Similarly, the combinations of antigen-specific IgG responses that were associated with protection from febrile malaria in immunoepidemiological studies (Fig 2) all targeted antigens operating at multiple distinct steps of invasion, rather than multiple antigens operating at the same step. Focusing combinatorial strategies on non-overlapping steps during invasion may therefore maximize the chance of synergistic effects.

Discussion

Malaria vaccine candidate identification has so far largely consisted of detailed preclinical studies targeting a single antigen at a time, with two significant detrimental consequences. Firstly, few antigens can be studied, leaving the majority of potential targets in the *P. falciparum* genome unexplored. Secondly, such single targets are particularly susceptible to failure due to allele-specific responses, as if variants in that antigen evolve which are not recognised by the dominant vaccine-induced response, there is nothing to prevent vaccine escape. Next-generation malaria vaccines will need to target multiple antigens, preferably in combinations that induce synergistic responses. Such a design would mimic what is now becoming clear about natural immunity to malaria, where the breadth of response to multiple antigens is a much stronger predictor of protection than the response to any single antigen (13). This study performed a systematic screen of 29 *P. falciparum* antigens alone and together, and complemented *in vitro* inhibition and mechanistic studies with investigation of immune responses in the field to prioritise candidates and combinations. Multiple targets were identified that induced antibodies which inhibited *P. falciparum* growth and several combinations of these antibodies were synergistic *in vitro*, mirroring immunoepidemiological data that combinations of antibodies against the same targets were associated with protection *in vivo* at a field site in Mali. This study also highlights the complexity of antibody interactions. For example, in *in vitro* invasion studies, anti-PfRh5 and anti-PfEBA181 IgG interact antagonistically at high levels of anti-Rh5 IgG but synergistically at low levels of anti-Rh5 IgG. Intriguingly, the latter scenario is consistent with seroepidemiological data which has shown that anti-RH5 IgG associates with malaria protection despite having relatively low reactivity (28).

Although screening 29 antigens in this manner is a significant step forward, it represents perhaps only 1/3 of the antigens that are exposed on the parasite surface during erythrocyte invasion. The number of antigens that could be screened was in part limited by the HEK293E

283 expression system. This system has several advantages, most significantly that by being
284 eukaryotic it is more likely to produce antigens that are functional and will therefore best mimic
285 their native counterparts. However, significant amounts of antigen (up to 1 mg) are required for
286 immunisation studies such as these, and in general only 70-80% of antigens can be expressed
287 at these levels in the HEK293E system (10, 32). The HEK293E expression system may also not
288 suit all antigens, so there is a risk of false negatives, as there is in any systematic screen. This
289 may explain the absence of inhibitory antibodies generated against MSP2, for example, which
290 has previously been extensively investigated as a blood-stage vaccine candidate (33).
291 Alternative eukaryotic expression systems such as the insect cell system used recently for
292 successful expression of PfRh5 (34), or the wheat germ cell-free system used for its binding
293 partner PfRIPR (35), may be required in addition to perform truly comprehensive blood stage
294 antigen screens. Testing for effective strain-transcendence is also a critical consideration. Now
295 that the true extent of global genomic variation has been revealed by large-scale genome
296 sequencing studies (6), it is apparent that there are several geographic regions that have
297 distinct genomic repertoires but for which there are no commonly available *in vitro* adapted
298 isolates for testing. Identification, expansion and distribution of *P. falciparum* isolates from these
299 areas, specifically East Africa, India/Bangladesh, and Papua New Guinea, will be an essential
300 step to enable more comprehensive assessment of strain-transcendence. In addition, efforts to
301 standardise growth inhibition assays need to focus on miniaturization, in order to allow testing of
302 a larger number of isolates when antibody volume is limiting, as it was here.
303
304 Despite these limitations, several new antigens and combinations were identified in this study.
305 As well as identifying novel targets, this work also suggests a logical rationale to guide the
306 selection of potentially synergistic combinations - targeting multiple independent steps in the
307 same pathway, in this case erythrocyte invasion. The mechanism by which a given combination
308 results in synergy is not known, but it has been previously suggested that kinetics could play a

role, where binding to some merozoite surface antigens might slow invasion down sufficiently to allow other antibodies to bind (36). This model certainly fits with some mechanisms uncovered by video microscopy, such as anti-EBA181 which appears to increase the duration of merozoite-erythrocyte contacts and show some evidence for synergy with anti-Rh5. However, further work is clearly required to truly understand the mechanisms of inhibition, and the strategy of targeting multiple steps is not the only viable approach, as recent studies of the AMA1-RON2 interaction that forms a complex late during erythrocyte invasion shows that in this case inhibiting both members of the same complex is more effective than targeting either alone (37).

Targeting multiple antigens will require parasites to simultaneously evolve variants in multiple antigens to avoid vaccine-induced immune responses, which should slow the emergence of resistance at the population level. Targeting antigens that operate at distinct steps in the same pathway offers an additional level of redundancy at the single parasites level by requiring individual merozoites to avoid inhibition of multiple temporally distinct steps. This same theoretical approach may be applied to other malaria vaccine targets, such as the recognition and invasion of hepatocytes by *Plasmodium* sporozoites for pre-erythrocytic stage vaccines, or gamete development within the *Anopheles* midgut for transmission blocking vaccines. A deeper understanding of all of these biological processes coupled with more systematic reverse vaccinology approaches will help further drive the development of the next generation of more complex, and more effective, malaria vaccine combinations.

Methods

Recombinant merozoite protein production

Recombinant extracellular domains of merozoite proteins were produced by transient transfection of HEK293 cells, as previously described (*11*). Culture supernatants were collected after 6 days and tested for expression of recombinant proteins by ELISA, using a mouse monoclonal antibody that binds the CD4 tag (OX68) to detect expressed protein.

Protein purification and quality assessment

Recombinant merozoite proteins were purified from pooled transfection supernatants using HisTrap HP columns (GE Healthcare). Proteins were eluted using an elution buffer containing 400 mM imidazole, then dialyzed against PBS (D-tube Dialyzer, Novagen). The concentration of protein samples was determined by absorbance at 280 nm, using *in silico* predicted extinction coefficients (DS Gene version 1.5, Accelrys), and quality assessed by ELISA and reducing SDS-PAGE.

Antibody purification and quality assessment

Rabbit polyclonal antibodies were raised against purified recombinant proteins by Cambridge Research Biochemicals after ethical assessment. Sera was tested for activity against the appropriate antigen by ELISA, then purified using a HiTrap Protein G HP column (GE Healthcare). Purified antibodies were dialyzed against PBS (or RPMI 1640 for invasion assays), tested for activity against the appropriate antigen by ELISA and quality assessed by reducing SDS-PAGE.

Parasite culture and GIA assays

3D7 and Dd2 parasites were cultured in human O+ erythrocytes. GIAs were carried out in round-bottom 96-well plates, with a culture volume of 100 µL per well at a hematocrit of 2%.

Synchronized parasites were incubated with antibodies for 24 hours at 37 °C before being stained with 1:5,000 SYBR Green I (Invitrogen) to detect parasite DNA (*12*). Invasion efficiency was calculated by comparing invasion in the presence of a given antibody concentration to invasion in the absence of antibodies. All experiments were carried out in triplicate.

Human Cohort Study

The details of the Malian prospective cohort study have been described (28), approved by ethical boards in Mali and the US, and registered on http://www.clinicaltrials.gov (number NCT01322581). Written, informed consent was obtained from adult participants and from the parents or guardians of participating children. For this study, malaria episodes were defined as an asexual parasite density by peripheral blood smear of >2500 parasites/μL, an axillary temperature of ≥37.5° C within 24 hours and no other cause of fever discernible by physical exam.

Immunoepidemiology

Plasma IgG levels against target antigens were determined by enzyme-linked immunosorbent assay (ELISA) as previously described (*26*), and outlined in detail in the Supplementary Information. In brief, plasma samples from each individual were tested in duplicate, alongside the same positive controls (hyperimmune plasma) and negative controls (unexposed donor plasma). ODs, adjusted for background, were converted to arbitrary units (AU) by dividing the test OD by the mean OD for negative controls plus 3 standard deviations and AU > 1 was defined a positive IgG response. A base Cox proportional hazards model was used to determine whether positive IgG responses to any of the 63 possible reactivity combinations was associated with a reduction in risk of clinical malaria, using time from first *P. falciparum* blood-stage inoculum (estimated as the mid-point between the last *Plasmodium*-PCR-negative visit and the first *Plasmodium*-PCR-positive visit) to first febrile malaria episode as the dependent

variable, and controlling for potential confounding variables (Table S3). *In vivo* parasite multiplication rates were estimated using qPCR-determined parasite density at the first PCR-positive visit and the number of days between the first *P. falciparum* blood-stage inoculum and the first smear-positive visit. Analyses were performed in R version 3.3.0 (http://www.R-project.org) or Prism version 5.0d (GraphPad Software).

Isobologram analyses

Dose-response assays were first carried out to obtain the 50% inhibitory concentration (IC_{50}) of the individual antibodies. Interactions were then assessed over a range of concentrations by a fixed-ratio method based on the IC_{50} values (*27*). Fractional IC_{50}s (FIC_{50}s) were calculated on the basis of the IC_{50}s obtained per assay for each antibody (the FIC_{50} is equal to the IC_{50} of antibody A in combination with antibody B/IC_{50} of antibody A alone) and used to plot isobolograms. An interaction index was calculated by summing the FIC_{50} derived from each of the two antibodies in any combination, and confidence intervals calculated using Monte Carlo simulation based on the error terms in the fitted IC_{50} curves.

Video Microscopy

Highly synchronous *P. falciparum* 3D7 late-stage schizonts were purified using a magnetic column (Miltenyi Biotec) and placed in a Secure-Seal hybridization chamber (Sigma-Aldrich) mounted on a glass slide. All live-cell experiments were performed in a homebuilt environmental chamber at 37 °C with humidified gas supply. Imaging was performed using a Nikon Eclipse TI-E inverted microscope through a Plan Apo λ 40× 0.95 N.A. dry objective (Nikon). Time-lapse videos were recorded on a Grasshopper3 GS3-U3-23S6M-C camera (Point Grey Research) at 4 frames per second. A custom MATLAB program was employed to perform image recording and statistical analysis.

Acknowledgments: Thanks to Prof. Stephen W. Wilson for providing support to GTP during completion of the project. We would like to thank all study subjects and staff involved in the epidemiological surveys in Mali. This work was supported by the Wellcome Trust (grant number 090851) and the Division of Intramural Research, National Institute of Allergy and Infectious Diseases, National Institutes of Health. TMT is supported in part by the Indiana Clinical and Translational Sciences Institute (Grant Number KL2 TR000163).

References

1. WorldHealthOrganisation (2015) *WHO World Malaria Report*, World Health Organisation.
2. Bhatt S*, et al.* (2015) The effect of malaria control on Plasmodium falciparum in Africa between 2000 and 2015. *Nature* 526(7572):207-211.
3. Ashley EA*, et al.* (2014) Spread of artemisinin resistance in Plasmodium falciparum malaria. *The New England journal of medicine* 371(5):411-423.
4. Rts SCTP (2015) Efficacy and safety of RTS,S/AS01 malaria vaccine with or without a booster dose in infants and children in Africa: final results of a phase 3, individually randomised, controlled trial. *Lancet* 386(9988):31-45.
5. Neafsey DE*, et al.* (2015) Genetic Diversity and Protective Efficacy of the RTS, S/AS01 Malaria Vaccine. *New Engl J Med* 373(21):2025-2037.
6. Malaria GENPfCP (2016) Genomic epidemiology of artemisinin resistant malaria. *eLife* 5.
7. Group MVF (2013) *Malaria Vaccine Technology Roadmap*.
8. Conway DJ (2015) Paths to a malaria vaccine illuminated by parasite genomics. *Trends in genetics : TIG* 31(2):97-107.
9. Hu G*, et al.* (2010) Transcriptional profiling of growth perturbations of the human malaria parasite Plasmodium falciparum. *Nature biotechnology* 28(1):91-98.
10. Crosnier C*, et al.* (2013) A library of functional recombinant cell surface and secreted Plasmodium falciparum merozoite proteins. *Molecular & cellular proteomics : MCP*.
11. Crosnier C*, et al.* (2011) Basigin is a receptor essential for erythrocyte invasion by Plasmodium falciparum. *Nature* 480(7378):534-537.
12. Wanaguru M, Crosnier C, Johnson S, Rayner JC, & Wright GJ (2013) Biochemical Analysis of the Plasmodium falciparum Erythrocyte-binding Antigen-175 (EBA175)-

Glycophorin-A Interaction: Implications for Vaccine Design. *The Journal of biological chemistry* 288(45):32106-32117.

13. Osier FH*, et al.* (2014) New antigens for a multicomponent blood-stage malaria vaccine. *Science translational medicine* 6(247):247ra102.

14. Durocher Y, Perret S, & Kamen A (2002) High-level and high-throughput recombinant protein production by transient transfection of suspension-growing human 293-EBNA1 cells. *Nucleic acids research* 30(2):E9.

15. Theron M, Hesketh RL, Subramanian S, & Rayner JC (2010) An adaptable two-color flow cytometric assay to quantitate the invasion of erythrocytes by Plasmodium falciparum parasites. *Cytometry A* 77(11):1067-1074.

16. Volkman SK*, et al.* (2007) A genome-wide map of diversity in Plasmodium falciparum. *Nat Genet* 39(1):113-119.

17. Douglas AD*, et al.* (2011) The blood-stage malaria antigen PfRH5 is susceptible to vaccine-inducible cross-strain neutralizing antibody. *Nat Commun* 2:601.

18. Bustamante LY*, et al.* (2013) A full-length recombinant Plasmodium falciparum PfRH5 protein induces inhibitory antibodies that are effective across common PfRH5 genetic variants. *Vaccine* 31(2):373-379.

19. Kadekoppala M, O'Donnell RA, Grainger M, Crabb BS, & Holder AA (2008) Deletion of the Plasmodium falciparum merozoite surface protein 7 gene impairs parasite invasion of erythrocytes. *Eukaryotic cell* 7(12):2123-2132.

20. Adams JH, Blair PL, Kaneko O, & Peterson DS (2001) An expanding ebl family of Plasmodium falciparum. *Trends in parasitology* 17(6):297-299.

21. Miller SK*, et al.* (2002) A subset of Plasmodium falciparum SERA genes are expressed and appear to play an important role in the erythrocytic cycle. *The Journal of biological chemistry* 277(49):47524-47532.

22. Reddy KS*, et al.* (2015) Multiprotein complex between the GPI-anchored CyRPA with PfRH5 and PfRipr is crucial for Plasmodium falciparum erythrocyte invasion. *Proceedings of the National Academy of Sciences of the United States of America* 112(4):1179-1184.

23. Volz JC*, et al.* (2016) Essential Role of the PfRh5/PfRipr/CyRPA Complex during Plasmodium falciparum Invasion of Erythrocytes. *Cell host & microbe* 20(1):60-71.

24. Nixon CP*, et al.* (2005) Antibodies to rhoptry-associated membrane antigen predict resistance to Plasmodium falciparum. *J Infect Dis* 192(5):861-869.

25. Ogutu BR*, et al.* (2009) Blood stage malaria vaccine eliciting high antigen-specific antibody concentrations confers no protection to young children in Western Kenya. *PloS one* 4(3):e4708.

26. Dreyer AM*, et al.* (2012) Passive immunoprotection of Plasmodium falciparum-infected mice designates the CyRPA as candidate malaria vaccine antigen. *J Immunol* 188(12):6225-6237.

27. Crompton PD*, et al.* (2010) A prospective analysis of the Ab response to Plasmodium falciparum before and after a malaria season by protein microarray. *Proceedings of the National Academy of Sciences of the United States of America* 107(15):6958-6963.

28. Tran TM*, et al.* (2014) Naturally acquired antibodies specific for Plasmodium falciparum reticulocyte-binding protein homologue 5 inhibit parasite growth and predict protection from malaria. *J Infect Dis* 209(5):789-798.

29. Fivelman QL, Adagu IS, & Warhurst DC (2004) Modified fixed-ratio isobologram method for studying in vitro interactions between atovaquone and proguanil or dihydroartemisinin against drug-resistant strains of Plasmodium falciparum. *Antimicrob Agents Chemother* 48(11):4097-4102.

30. Weiss GE*, et al.* (2015) Revealing the sequence and resulting cellular morphology of receptor-ligand interactions during Plasmodium falciparum invasion of erythrocytes. *PLoS Pathog* 11(2):e1004670.

31. Crick AJ*, et al.* (2013) An automated live imaging platform for studying merozoite egress-invasion in malaria cultures. *Biophysical journal* 104(5):997-1005.

32. Zenonos ZA*, et al.* (2015) Basigin is a druggable target for host-oriented antimalarial interventions. *Journal of Experimental Medicine* 212(8):1145-1151.

33. McCarthy JS*, et al.* (2011) A phase 1 trial of MSP2-C1, a blood-stage malaria vaccine containing 2 isoforms of MSP2 formulated with Montanide(R) ISA 720. *PloS one* 6(9):e24413.

34. Hjerrild KA*, et al.* (2016) Production of full-length soluble Plasmodium falciparum RH5 protein vaccine using a Drosophila melanogaster Schneider 2 stable cell line system. *Scientific reports* 6:30357.

35. Ntege EH*, et al.* (2016) Identification of Plasmodium falciparum reticulocyte binding protein homologue 5-interacting protein, PfRipr, as a highly conserved blood-stage malaria vaccine candidate. *Vaccine* 34(46):5612-5622.

36. Saul A (1987) Kinetic constraints on the development of a malaria vaccine. *Parasite immunology* 9(1):1-9.

37. Srinivasan P*, et al.* (2014) Immunization with a functional protein complex required for erythrocyte invasion protects against lethal malaria. *Proceedings of the National Academy of Sciences of the United States of America* 111(28):10311-10316.

38. Bell A (2005) Antimalarial drug synergism and antagonism: mechanistic and clinical significance. *FEMS microbiology letters* 253(2):171-184.

Figure Legends

Figure 1. Systematic screening of antibodies to *P. falciparum* antigens for cross-strain activity. 3D7 (black bars) and Dd2 (grey bars) strains of *P. falciparum* were grown for 48 hours in *in vitro* culture in the presence of purified rabbit polyclonal IgG raised against members of a panel of recombinant merozoite protein ectodomains. Bars represent mean growth relative to positive control wells lacking antibodies, and error bars represent standard deviation (n=3). Merozoite ectodomains are grouped by their known or predicted subcellular location.

Figure 2. Antigens are targets of natural IgG responses that are associated with protection from malaria in specific combinations. A) IgG reactivity against PfCyRPA, PfEBA181, PfMSRP5, PfRAMA or PfSERA9 in plasma samples from 351 Malians across age groups. Shown is background-subtracted optical density (OD 450 nm) by ELISA. Boxes enclose interquartile range, central lines represent medians, whiskers indicate the 5-95 percentile, and dots are outliers. B) Seroprevalence of IgG with AU (arbitrary units) of >1 against all antigens across age groups. 'AU of 1' is defined as the mean OD value plus 3 standard deviations for 24 malaria-naïve U.S. donors. C) A Cox regression model was used to evaluate the effect of different combinations of antigen-specific IgG responses on the risk of the first febrile malaria episode of the season using time of first PCR-detectable *P. falciparum* blood-stage infection as the start time for febrile malaria risk analysis. Shown are forest plots for the most significant combinations that did not include PfRh5.

Figure 3. Combinatorial screening reveals antibody pairs with synergistic effects. Isobolograms showing the combined effect of fixed ratio mixtures (5:0, 4:1, 3:2, 2:3, 1:4 and 0:5) of purified polyclonal antibodies on erythrocyte invasion by *P. falciparum* 3D7. In each case X and Y axes represent the FIC_{50} values associated with the two antibodies in each combination.

Dashed lines represent the expected result under Loewe additivity (sum of FIC_{50}s equal to 1). Points below this line are suggestive of synergistic inhibition, while points above it suggest antagonistic inhibition (38).

Figure 4. Video microscopy of erythrocyte invasion reveals discrete roles for candidate antigens. >40 egress events were recorded in the presence of IgG against each target, and a range of invasion-related phenotypes quantitated. A) Number of merozoite contacts that occur after each egress event. B) Time taken (s) between merozoite contact and erythrocyte deformation, sometimes referred to as pre-invasion, quantitated for merozoites that went on to productively invade erythrocytes (invaders) and those that did not (non-invaders). Total number of events analysed in A and B: control – 63, anti-PfMSRP5 – 65, anti-PfEBA181 – 49, anti-PfSERA9 – 53, anti-PfRh5 – 50, anti-PfRAMA – 55, anti-PfCyRPA - 52. C) Examples of deformation scores from 0 (no deformation) to 3 (strong deformation (*26*)). D) Range of deformation scores for every merozoite-erythrocyte interaction, quantitated for both invaders and non-invaders. E) Number of deformation events that take place after each egress event. Asterisks represent probability thresholds: * = $p < 0.06$, ** = $p < 0.001$, *** = $p < 0.0005$. F) Schematic summarising the data in this study for each antigen: the phase of invasion they function in, as determined by video microscopy (numbered black boxes 1 – 4); the synergistic (dark blue arrows), antagonistic (black bars) and mixed synergistic/antagonistic interactions (purple diamonds) between antibodies targeting these antigens based on isobologram analyses; the immunoprotective combinations of antigens revealed in the Malian cohort study (connected circles); and the physical location of the proteins on merezoites (beige boxes).

Figure 1.

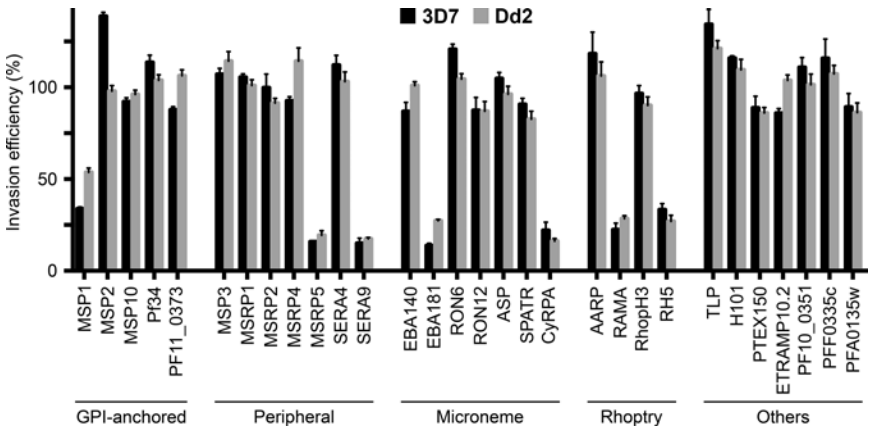
3D7
Dd2
Invasion efficiency (%)
100
50
0
MSP1
MSP2
MSP10
Pf34
PF11_0373
MSP3
MSRP1
MSRP2
MSRP4
MSRP5
SERA4
SERA9
EBA140
EBA181
RON6
RON12
ASP
SPATR
CyRPA
AARP
RAMA
RhopH3
RH5
TLP
H101
PTEX150
ETRAMP10.2
PF10_0351
PFF0335c
PFA0135w
GPI-anchored
Peripheral
Microneme
Rhoptry
Others

562 **Figure 2.**

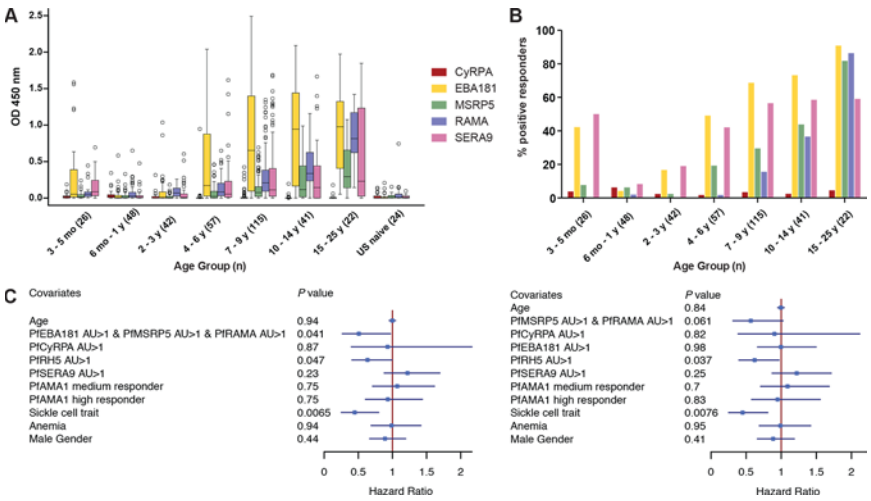
A
OD 450 nm
CyRPA
EBA181
MSRP5
RAMA
SERA9
3 - 5 mo (26)
6 mo - 1 y (46)
2 - 3 y (42)
4 - 6 y (57)
7 - 9 y (115)
10 - 14 y (41)
15 - 25 y (22)
US naive (24)
Age Group (n)
B
% positive responders
Age Group (n)
C
Covariates
P value
Age 0.94
PfEBA181 AU>1 & PfMSRP5 AU>1 & PfRAMA AU>1 0.041
PfCyRPA AU>1 0.87
PfRH5 AU>1 0.047
PfSERA9 AU>1 0.23
PfAMA1 medium responder 0.75
PfAMA1 high responder 0.75
Sickle cell trait 0.0065
Anemia 0.94
Male Gender 0.44
Hazard Ratio
Covariates
P value
Age 0.84
PfMSRP5 AU>1 & PfRAMA AU>1 0.061
PfCyRPA AU>1 0.82
PfEBA181 AU>1 0.98
PfRH5 AU>1 0.037
PfSERA9 AU>1 0.25
PfAMA1 medium responder 0.7
PfAMA1 high responder 0.83
Sickle cell trait 0.0076
Anemia 0.95
Male Gender 0.41
Hazard Ratio

563 **Figure 3.**

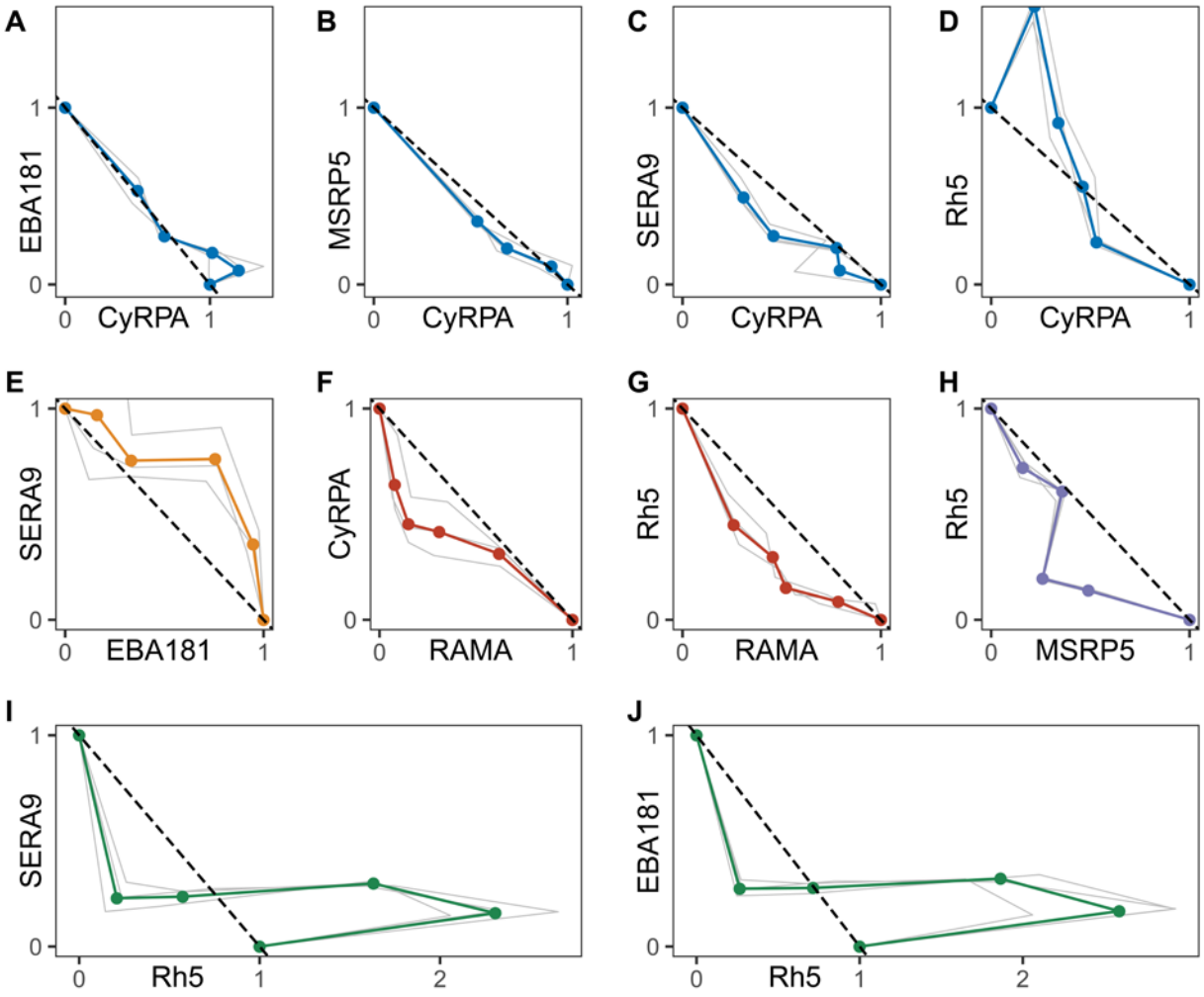
A
EBA181
CyRPA
B
MSRP5
CyRPA
C
SERA9
CyRPA
D
Rh5
CyRPA
E
SERA9
EBA181
F
CyRPA
RAMA
G
Rh5
RAMA
H
Rh5
MSRP5
I
SERA9
Rh5
J
EBA181
Rh5

564 **Figure 4.**

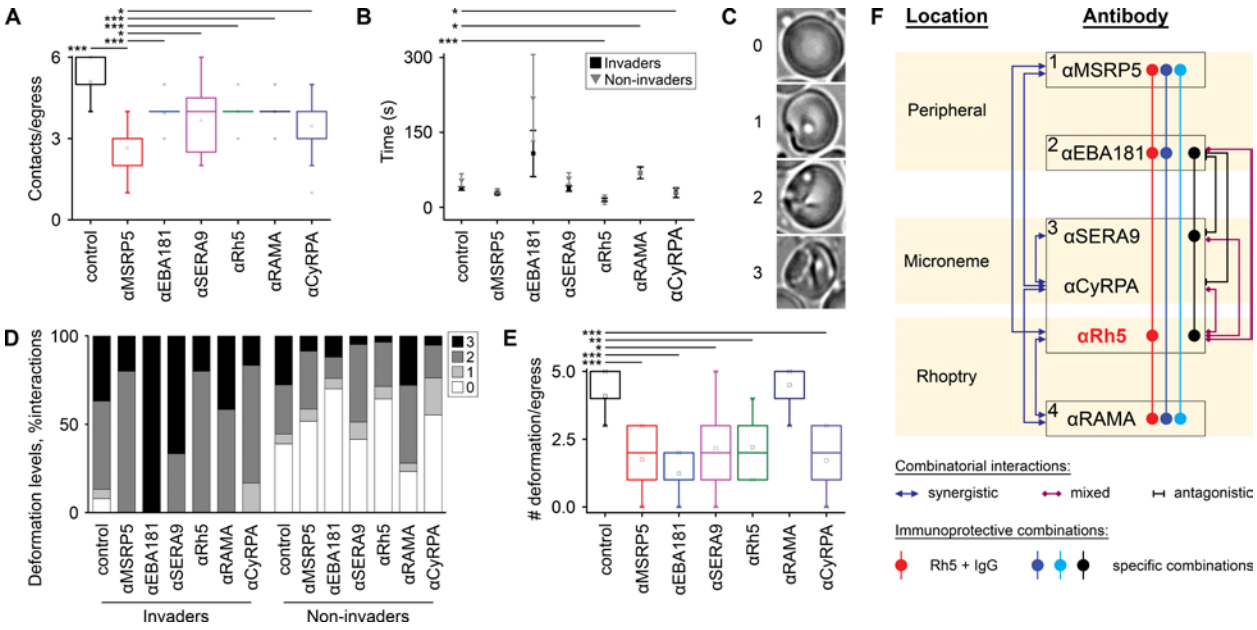
A
Contacts/egress
control
αMSRP5
αEBA181
αSERA9
αRh5
αRAMA
αCyRPA
B
Time (s)
Invaders
Non-invaders
C
D
Deformation levels, %interactions
Invaders
Non-invaders
E
deformation/egress
F
Location
Antibody
Peripheral
Microneme
Rhoptry
αMSRP5
αEBA181
αSERA9
αCyRPA
αRh5
αRAMA
Combinatorial interactions:
synergistic
mixed
antagonistic
Immunoprotective combinations:
Rh5 + IgG
specific combinations

SUPPLEMENTARY INFORMATION FOR

Systematic screening of antigens identifies synergistic malaria vaccine combinations

Leyla Y. Bustamante, Gareth T. Powell, Yen-Chun Lin, Michael D. Macklin, Nadia Cross, Alison Kemp, Paula Cawkill, Theo Sanderson, Cecile Crosnier, Nicole Muller-Sienerth, Ogobara K. Doumbo, Boubacar Traore, Peter D. Crompton, Pietro Cicuta, Tuan M. Tran, Gavin J. Wright, Julian C. Rayner

Correspondence to: julian.rayner@sanger.ac.uk

This file includes:

Materials and Methods

Legends for Supplementary Movies

Legends for Supplementary Figures

Materials and Methods:

Recombinant merozoite protein production

Recombinant extracellular domains of merozoite proteins fused with rat CD4 domains 3 and 4 and hexahistidine tags were produced by transient transfection of mammalian cell culture using PEI, as previously described (*11*). Briefly, HEK293E or HEK293F cells, cultured in suspension in Freestyle 293 media (Gibco) supplemented with (HEK293E cells only) 1% fetal calf serum (Sigma), penicillin (100 units/mL, Sigma), streptomycin (0.1 mg/mL, Sigma) and geneticin (50 µg/mL, Sigma), were transfected with an expression plasmid encoding the protein of interest using linear 25 kDa PEI (Polyscience) mixed in a ratio of 2:1 (PEI:DNA, w/w) in 2 mL of unsupplemented media. Transfected cell culture supernatants were collected after 6 days and

tested for expression of recombinant proteins by ELISA, using nickel-coated microtiter plates (Qiagen) to immobilize hexahistidine-tagged proteins and a mouse monoclonal antibody that binds the CD4 tag (OX68) to detect expressed protein. *In silico* predictions of molecular weight, isoelectric point, aliphatic index and grand average of hydropathicity index were calculated using DS Gene (version 1.5, Accelrys).

Protein purification and quality assessment

Recombinant merozoite proteins were purified from pooled transfection supernatants by IMAC using HisTrap HP columns (GE Healthcare). Proteins were eluted from the column using an elution buffer containing 400 mM imidazole, then dialyzed against PBS (D-tube Dialyzer, Novagen). The concentration of protein samples was determined by absorbance at 280 nm, using *in silico* predicted extinction coefficients (DS Gene version 1.5, Accelrys). Quality and quantity of each purified sample was assessed by ELISA and reducing SDS-PAGE, using premade NuPAGE 4-12% Bis-Tris buffered polyacrylamide gels (Novex) and MOPS running buffer. Proteins were visualized using SYPRO Orange dye (Sigma) and a Typhoon (GE Healthcare) laser scanner. Images were adjusted for brightness and contrast in Abode Photoshop CS2.

Antibody purification and quality assessment

Bespoke rabbit polyclonal antibodies raised against the purified recombinant proteins were prepared by Cambridge Research Biochemicals after ethical assessment. Rabbits were immunized 4 times with a total amount of 0.3–0.6 mg of each purified antigen and exsanguinated after 77 days. Each harvested antibody sera was tested for activity against the appropriate antigen by ELISA, then purified using a HiTrap Protein G HP column (GE Healthcare). Total IgG antibodies were eluted from the column using 0.1 M glycine-HCl pH 2.7 and immediately neutralized with 2M Tris-HCl pH 9.5. Purified antibodies were dialyzed against

PBS and the concentration of IgG determined by absorbance at 280 nm. Each purified polyclonal IgG sample was tested for activity against the appropriate antigen by ELISA, with 500 ng target protein immobilized in each well. The quality of purification was assessed by reducing SDS-PAGE. Polyclonal antibody samples were dialyzed against RPMI 1640, without phenol red (Gibco), prior to use in invasion assays.

Parasite culture and GIA assays

3D7 and Dd2 parasites were obtained from MR4 (www.mr4.org). *P. falciparum* parasite strains were cultured in human O+ erythrocytes at 5% hematocrit in complete medium (RPMI-1640 supplemented with Albumax), under an atmosphere of 1% O_2, 3% CO_2, and 96% N_2. Use of erythrocytes from human donors for *P. falciparum* culture was approved by the NHS Cambridgeshire 4 Research Ethics Committee, and all donors supplied written informed consent. GIA assays were carried out in round-bottom 96-well plates, with a culture volume of 100 µL per well at a hematocrit of 2%. Parasites were synchronized at early stages with 5% (w/v) D-sorbitol (Sigma), trophozoite stage parasites were incubated in the presence or absence of antibodies for 24 hours at 37 °C inside a static incubator culture chamber (VWR), gassed with 1% O_2, 3% CO_2, and 96% N_2. All antibodies were dialyzed into RPMI before addition into GIA assays. At the end of the incubation period, cultures were harvested and fixed, and parasitized erythrocytes were stained with 1:5,000 SYBR Green I (Invitrogen), as described previously (*12*). SYBR Green I stained samples were excited with a 488 nm UV laser on a BD Calibur flow cytometer (BD Biosciences) and detected with a 530/30 filter. BD FACS Diva software (BD Biosciences) was used to analyze 50,000 events for each sample. FSC and SSC voltages of 423 and 198, respectively, and a threshold of 2,000 on FSC were applied to gate the erythrocyte population. The data collected were further analyzed with FlowJo (Tree Star). Invasion efficiency was calculated by comparing invasion in the presence of a given antibody

concentration to invasion in the absence of antibodies. All experiments were carried out in triplicate. GraphPad Prism (GraphPad Software) was used to plot the parasitemia data.

Cross-reactivity

To assess the specificity of the polyclonal, purified anti-EBA181, anti-MSRP5 and anti-SERA9 antibodies were tested for activity against the recombinant extracellular domains of other EBA, MSP7-like and SERA family members, respectively, by ELISA. Four members of the SERA family were not included in the assay because we were unable to produce them by transient transfection. The purified antibodies were diluted and mixed with or without purified, recombinant CD4 tag-only protein at a ratio of 1:10 antibody:tag protein (w/w; final antibody concentration 100 µg/mL) in order to eliminate activity against the tag domains common to all ectodomains. The antibodies were incubated at room temperature for 30 minutes before use. The undepleted and depleted antibodies were tested for activity against recombinant, biotinylated extracellular domains of EBA, MSP7-like and SERA family proteins, immobilized on the surface of streptavidin-coated microtiter plates, by ELISA. A high antibody concentration (100 µg/mL) was used in the assay in order to detect any low titer cross-reactivity.

Human Cohort Study

The details of the Malian prospective cohort study have been described (43). The Ethics Committee of the Faculty of Medicine, Pharmacy and Dentistry at the University of Sciences, Technique and Technology of Bamako, and the Institutional Review Board of the National Institute of Allergy and Infectious Diseases, National Institutes of Health approved the Malian cohort study, which is registered on http://www.clinicaltrials.gov (number NCT01322581). Written, informed consent was obtained from adult participants and from the parents or guardians of participating children. For this study, malaria episodes were defined as an asexual

parasite density by peripheral blood smear of >2500 parasites per µL, an axillary temperature of ≥37.5 °C within 24 hours and no other cause of fever discernible by physical exam.

Determination of the first-detectable blood-stage infection

Blood was collected by finger stick for dried blood spots and thick blood smears during scheduled clinic visits occurring at two-week intervals over 7 months or during unscheduled acute visits. Smears were stained with Giemsa and read contemporaneously if the participant demonstrated signs or symptoms of illness. Individuals with positive smears at any level of *Plasmodium* parasitemia were treated according to the National Malaria Control Program guidelines in Mali. At the completion of the first year of the study, dried blood spots and the remainder of the smears were retrospectively assessed for the presence of parasitemia in chronological order until the first *P. falciparum*-positive sample by PCR. Parasite densities were estimated by quantitative PCR (qPCR) from DNA extracted from dried blood spots as previously described (1).

Immunoepidemiology

Plasma IgG levels against PfCyRPA, PfEBA181, PfMSRP5, PfRAMA, PfSERA9, and rat Cd4 domains 3+4 were determined by enzyme-linked immunosorbent assay (ELISA) as previously described (*43*) except that PBS was substituted for HBS. Plasma samples from each individual were always tested in duplicate against all five antigens concurrently in consecutive wells of the same plate. The same positive controls (hyperimmune plasma) known to react to *P. falciparum* antigens and negative controls (unexposed donor plasma) were run in duplicate on each plate. Identical positive controls allowed for normalization between plates to account for plate-to-plate and day-to-day variation. Average background optical density (OD) from rat-Cd4-coated wells was subtracted from the average OD for *P. falciparum* antigen-coated wells to obtain antigen-specific OD values. Plasma samples obtained from 24 U.S. residents with no history of malaria

and no travel to malaria-endemic countries were used as negative controls. ODs were converted to arbitrary units (AU) by dividing the test OD by the mean OD for 24 malaria-naïve U.S. donors plus 3 standard deviations. AU > 1 defined a positive IgG response. IgG reactivity data for PfRH5 and PfAMA1 included in subsequent analyses have been described previously (*43*).

A base Cox proportional hazards model was used to determine whether positive IgG responses to any of the 63 possible reactivity combinations for PfCyRPA, PfEBA181, PfMSRP5, PfRAMA, PfSERA9, and PfRH5 associated with a reduction in risk of clinical malaria in 63 separate analyses. Specifically, the dependent variable was time from first *P. falciparum* blood-stage inoculum (estimated as the mid-point between the last *Plasmodium*-PCR-negative visit and the first *Plasmodium*-PCR-positive visit) to first febrile malaria episode. Potential confounding variables included in all base models were age as a continuous variable and sickle cell trait, anemia status, and gender as categorical variables. The Cox proportional hazard assumption was tested with the cox.zph function in the *survival* package (44). Hazard ratios, 95% confidence intervals, *P* values, Benjamini-Hochberg adjusted *P* values (false discovery rates), and *P* values for assumption testing for all possible combinations are in Table S3. For the combinations that demonstrated statistically significant reduction in malaria risk, additional covariates were added which included IgG responses to any antigen not included in the combination of interest and IgG reactivity to PfAMA1 (as terciles ordered by low, medium and high responders), which served as a proxy for previous malaria exposure. The *in vivo* parasite multiplication rate (PMR) was approximated by dividing the qPCR-determined parasite density at the first *Plasmodium*-PCR-positive visit by the number of days between the first *P. falciparum* blood-stage inoculum (described above) and the first *Plasmodium*-PCR-positive visit. For each IgG reactivity combination, the $\log_{10}$(PMR+1) was compared between positive and negative responders by Wilcoxon test and using a logistic regression model. For the latter, PMR

(dichotomized using the median PMR) was the response variable, and IgG response (positive/negative), age (in years), sickle cell trait, anemia status, and gender were independent variables (Table S4). Analyses involving PMRs were limited to antigen combinations for which there were at least six positive IgG responders to minimize spurious associations. Analyses were performed in R version 3.3.0 (http://www.R-project.org) or Prism version 5.0d (GraphPad Software).

Isobologram analyses

Dose-response assays were first carried out to obtain the 50% inhibitory concentration (IC_{50}) of the individual antibodies. Interactions were then assessed over a range of concentrations by a fixed-ratio method based on the IC_{50} values (*32*). Briefly, antibody dilutions were made to allow the IC_{50} of the individual antibodies to fall at about the fourth twofold serial dilution. Stock solutions were then prepared at 5 times the IC_{50} of each antibody. Solutions were combined at fixed ratios of 5:0, 4:1, 3:2, 2:3, 1:4 and 0:5 for antibody A-antibody B. These starting solutions were serially diluted across six two-fold dilutions. The plates were processed at the end of the incubation period (24h), cultures were harvested and fixed, and parasitized erythrocytes were stained with 1:5,000 SYBR Green I (Invitrogen) and analyzed as described above. Fractional IC_{50}s (FIC_{50}s) were calculated on the basis of the IC_{50}s obtained per assay for each antibody (the FIC_{50} is equal to the IC_{50} of antibody A in combination with antibody B/IC_{50} of antibody A alone). The mean sums of the FIC_{50}s were calculated for all of the combinations tested and were based on the results obtained with fixed ratios of 4:1, 3:2, 2:3, 1:4.

Video Microscopy

Imaging was performed using a Nikon Eclipse TI-E inverted microscope through a Plan Apo λ 40× 0.95 N.A. dry objective (Nikon). For the bright field imaging, a halogen lamp with red filter is used as the light source. Time-lapse videos were recorded on a Grasshopper3 GS3-U3-23S6M-

C camera (Point Grey Research) at 4 frames per second. For live-cell imaging, highly synchronous *P. falciparum* 3D7 late-stage schizonts were purified using a magnetic column (Miltenyi Biotec). After purification, *P. falciparum* cultures were resuspended at 4% hematocrit and diluted to 0.2% in complete medium to provide an optimal cell density, then incubated at 37 °C to allow for recovery. 25 µL of volume of this mixture was mixed with 25 µL of invasion inhibitory antibodies, and placed in a Secure-Seal hybridization chamber (Sigma-Aldrich) mounted on a glass slide. All live-cell experiments were performed in a homebuilt environmental chamber at 37 °C with humidified gas supply (96% N_2, 1% O_2, and 3% CO_2). A custom MATLAB program was employed to perform image recording and statistical analysis.

Legends for Supplementary Movies:

Movie S1 – Positive control. Representative video microscopy file of *P. falciparum* erythrocyte invasion in the absence of any antibody. Purified schizonts were incubated with uninfected erythrocytes and recorded as described in Materials and Methods. The movie is annotated to illustrate merozoite contact, deformation and invasion. Data presented in Figure 4 contains the total data from >50 egress events for this condition.

Movie S2 – Anti-MSRP5. Representative video microscopy file of *P. falciparum* erythrocyte invasion in the presence of 5.2 mg/ml final concentration of anti-PfMSRP5. Purified schizonts were incubated with uninfected erythrocytes, plus antibody, and recorded as described in Materials and Methods. The movie is annotated to illustrate merozoite contact, deformation and invasion. Data presented in Figure 4 contains the total data from >50 egress events for this condition.

Movie S3 – Anti-EBA181. Representative video microscopy file of *P. falciparum* erythrocyte invasion in the presence of 4.8 mg/ml final concentration of anti-PfEBA181. Purified schizonts were incubated with uninfected erythrocytes, plus antibody, and recorded as described in Materials and Methods. The movie is annotated to illustrate merozoite contact, deformation and invasion. Data presented in Figure 4 contains the total data from >50 egress events for this condition.

Movie S4 – Anti-PfRh5. Representative video microscopy file of *P. falciparum* erythrocyte invasion in the presence of 2.5 mg/ml final concentration of anti-PfRh5. Purified schizonts were incubated with uninfected erythrocytes, plus antibody, and recorded as described in Materials and Methods. The movie is annotated to illustrate merozoite contact, deformation and invasion. Data presented in Figure 4 contains the total data from >50 egress events for this condition.

Movie S5 – Anti-CyRPA. Representative video microscopy file of *P. falciparum* erythrocyte invasion in the presence of 7.5 mg/ml final concentration of anti-PfCyRPA. Purified schizonts were incubated with uninfected erythrocytes, plus antibody, and recorded as described in Materials and Methods. The movie is annotated to illustrate merozoite contact, deformation and invasion. Data presented in Figure 4 contains the total data from >50 egress events for this condition.

Movie S6 – Anti-SERA9. Representative video microscopy file of *P. falciparum* erythrocyte invasion in the presence of 4.9 mg/ml final concentration of anti-PfSERA9 Purified schizonts were incubated with uninfected erythrocytes, plus antibody, and recorded as described in Materials and Methods. The movie is annotated to illustrate merozoite contact, deformation and invasion. Data presented in Figure 4 contains the total data from >50 egress events for this condition.

Movie S7 – Anti-RAMA. Representative video microscopy file of *P. falciparum* erythrocyte invasion in the presence of 6.0 mg/ml final concentration of anti-PfRAMA. Purified schizonts were incubated with uninfected erythrocytes, plus antibody, and recorded as described in Materials and Methods. The movie is annotated to illustrate merozoite contact, deformation and invasion. Data presented in Figure 4 contains the total data from >50 egress events for this condition.

Legends for Supplementary Figures:

Figure S1. Antigen quality assessment by SDS-PAGE.
Composite image of reducing SDS-PAGE gels showing samples of each recombinant ectodomain antigen (1 µg, determined by absorbance at 285 nm), after nickel column purification, arranged in order of descending predicted molecular weight. In most cases, the low expression level of the antigen necessitated processing of large volumes of tissue culture supernatant; this resulted in the retention of non-specfic proteins, such as serum albumin. The presence of the desired antigen in each purified sample was determined by ELISA using tag-specific antibodies before immunisation. 'M' – protein markers.

Figure S2. Antigen expression and corresponding antibody titers.
Graphs showing the expression level (nmoles purified protein/L transfection supernatant) of each antigen produced at large scale (black bars) and the titer (µg/mL, y-axis) of the corresponding purified, polyclonal antibodies raised against them, determined by ELISA (grey bars).

Figure S3. Limited cross-reactivity of anti-PfMSRP5 polyclonal antibodies with PfMSP7. Representative ELISA results using purified polyclonal antibodies (100 µg/mL) raised against (A) PfEBA181, (B) PfMSRP5 or (C) PfSERA9 to detect cross-reactivity with other members of the EBA, MSP7 or SERA families, respectively. The antibodies were tested with (black bars) or without (grey bars) depletion of activity against the tag fused to each recombinant protein immobilized on the microtiter plates (compare black and grey bars marked in A-C). These results show limited cross-reactivity of anti-PfMSRP5 antibodies to PfMSP7 and no detectable cross-reactivity of anti-PfSERA9 or anti-PfEBA181 antibodies. Average absorbance at 405 nm (n = 3); error bars represent standard deviation.

Figure S4. Strong, strain transcending dose-dependent inhibition of growth by antibodies raised against five new blood stage vaccine candidates. Graphs showing results of growth inhibition assays performed using either 3D7 (open circles) or Dd2 (black circles) strains and with increasing concentration of anti-PfSERA9 (A), anti-PfMSRP5 (B), anti-PfEBA181 (C), anti-PfCyRPA (D), or anti-PfRAMA (E) purified polyclonal antibodies added to the culture media. Both strains of parasite were strongly inhibited by all six polyclonal antibodies, although a small difference in efficacy was observed for anti-PfEBA181, anti-PfCyRPA and anti-PfRAMA. Circles represent mean values (n = 3); error bars represent standard error. Lack of strain specificity for anti-PfRh5 has been reported previously by multiple groups (*14, 15)* (3), and anti-PfCyRPA has also previously shown to have a strain-transcending protective effect (*19*) (4). By contrast, antibodies against stain-specific targets such as AMA1 have clear differences in efficacy between strains (*15*).

Figure S5. Confidence intervals for synergy/antagonism in antibody combinations. Dose-response data was analysed to calculate an interaction index, calculated as the sum of the two FIC_{50} values for each ratio. Confidence interval were computed for the interaction indices by

propagating the errors in the logIC_{50} values by Monte Carlo simulation. Antibody combinations are shown on the y axis with a ratio given for the proportions in which the first and second antibodies are mixed, while the interaction index is shown on the x-axis. Interaction indices >1 represent antagonism while those <1 represent synergy.

Figure S1.

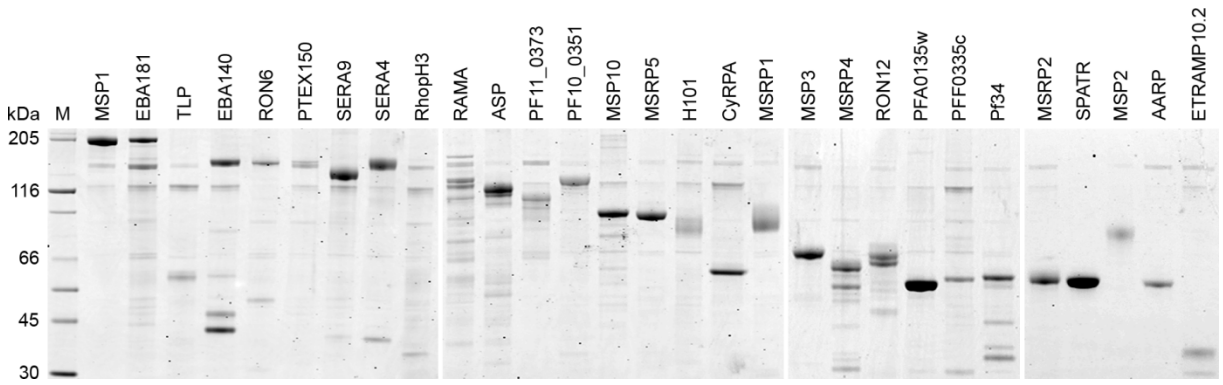
kDa
M
205
116
66
45
30
MSP1
EBA181
TLP
EBA140
RON6
PTEX150
SERA9
SERA4
RhopH3
RAMA
ASP
PF11_0373
PF10_0351
MSP10
MSRP5
H101
CyRPA
MSRP1
MSP3
MSRP4
RON12
PFA0135w
PFF0335c
Pf34
MSRP2
SPATR
MSP2
AARP
ETRAMP10.2

287 **Figure S2.**

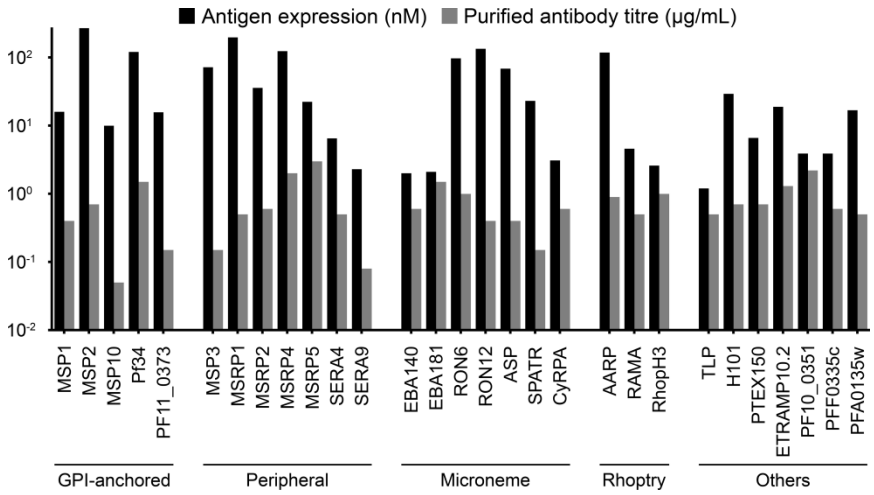

Figure S3.

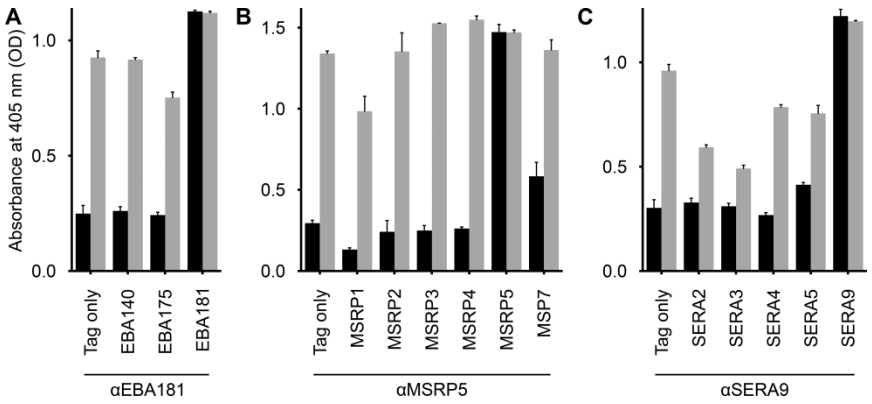
A
B
C
Absorbance at 405 nm (OD)
1.0
0.5
0.0
1.5
1.0
0.5
0.0
1.0
0.5
0.0
Tag only
EBA140
EBA175
EBA181
αEBA181
Tag only
MSRP1
MSRP2
MSRP3
MSRP4
MSRP5
MSP7
αMSRP5
Tag only
SERA2
SERA3
SERA4
SERA5
SERA9
αSERA9

289 **Figure S4.**

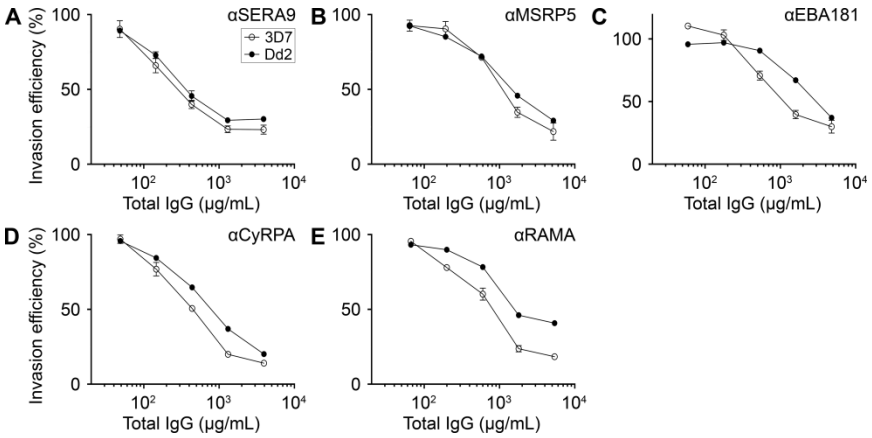

Figure S5.

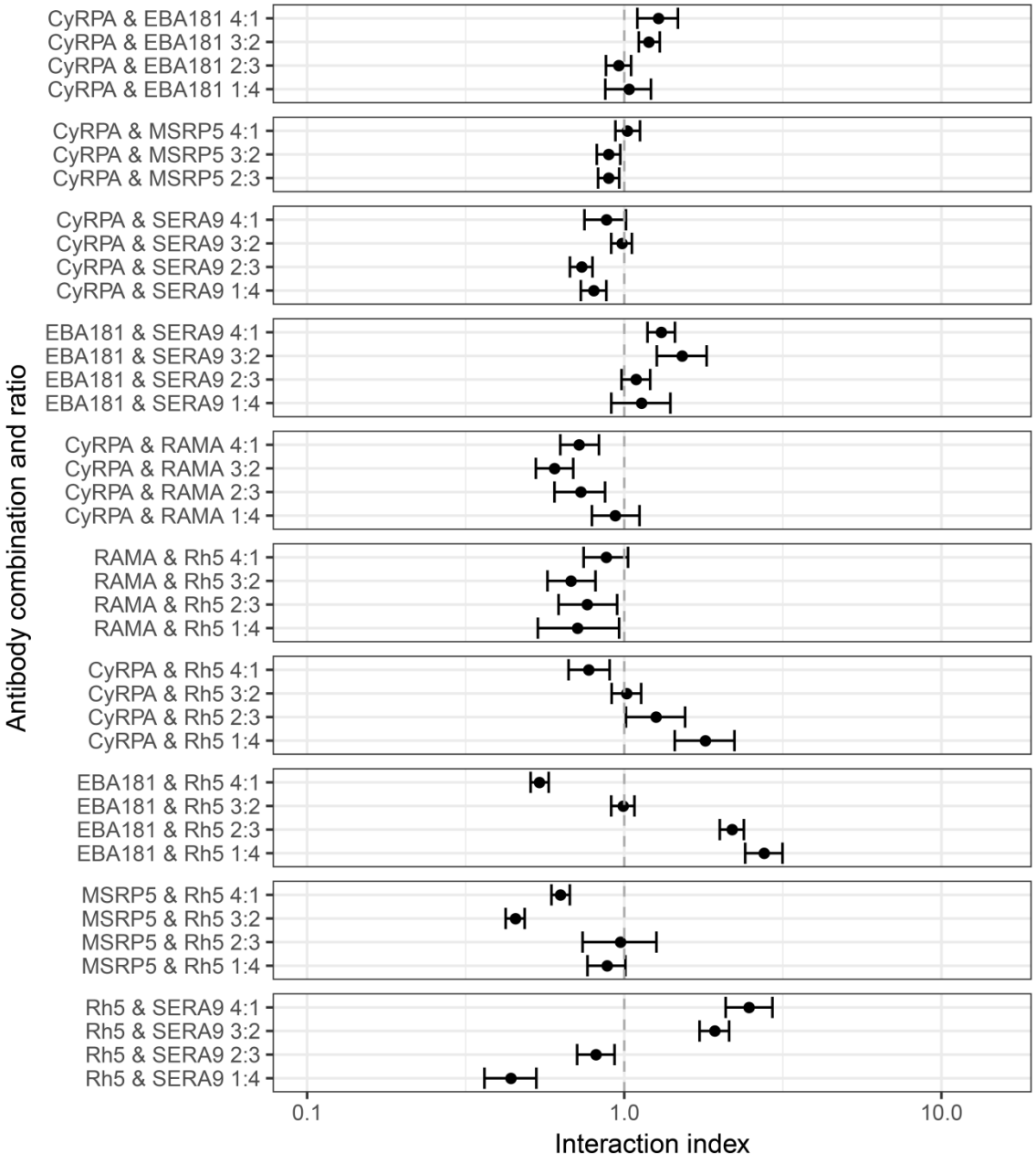
CyRPA & EBA181 4:1
CyRPA & EBA181 3:2
CyRPA & EBA181 2:3
CyRPA & EBA181 1:4
CyRPA & MSRP5 4:1
CyRPA & MSRP5 3:2
CyRPA & MSRP5 2:3
CyRPA & SERA9 4:1
CyRPA & SERA9 3:2
CyRPA & SERA9 2:3
CyRPA & SERA9 1:4
EBA181 & SERA9 4:1
EBA181 & SERA9 3:2
EBA181 & SERA9 2:3
EBA181 & SERA9 1:4
CyRPA & RAMA 4:1
CyRPA & RAMA 3:2
CyRPA & RAMA 2:3
CyRPA & RAMA 1:4
RAMA & Rh5 4:1
RAMA & Rh5 3:2
RAMA & Rh5 2:3
RAMA & Rh5 1:4
CyRPA & Rh5 4:1
CyRPA & Rh5 3:2
CyRPA & Rh5 2:3
CyRPA & Rh5 1:4
EBA181 & Rh5 4:1
EBA181 & Rh5 3:2
EBA181 & Rh5 2:3
EBA181 & Rh5 1:4
MSRP5 & Rh5 4:1
MSRP5 & Rh5 3:2
MSRP5 & Rh5 2:3
MSRP5 & Rh5 1:4
Rh5 & SERA9 4:1
Rh5 & SERA9 3:2
Rh5 & SERA9 2:3
Rh5 & SERA9 1:4
Antibody combination and ratio
0.1
1.0
10.0
Interaction index